Tumorigenesis and Neoplastic Progression

Irs2 Inactivation Suppresses Tumor Progression in Pten$^{+/-}$ Mice

Matthias Szabolcs,*[†] Megan Keniry,*
Laura Simpson,* Latarsha J. Reid,*
Susan Koujak,* Sarah C. Schiff,*
Giselle Davidian,* Scott Licata,*
Sofia Gruvberger-Saal,* Vundavalli V.V.S. Murty,*[†]
Subhadra Nandula,*[†] Argiris Efstratiadis,*[‡]
Jake A. Kushner,[§] Morris F. White,[¶]
and Ramon Parsons*

From the Institute for Cancer Genetics and the Departments of*
Pathology[‡] and Genetics and Development,[‡] College of Physicians
and Surgeons, Columbia University, New York, New York; the
Division of Endocrinology,[§] Children's Hospital of Philadelphia,
University of Pennsylvania, Philadelphia, Pennsylvania; and the
Division of Endocrinology,[¶] Howard Hughes Medical Institute,
Children's Hospital, Harvard Medical School,
Boston, Massachusetts

Mutations in the phosphatase and tensin homologue (PTEN)/phosphatidylinositol-3 kinase-α (PI3K) signaling pathway are frequently found in human cancer. In addition, Pten$^{+/-}$ mice develop tumors in multiple organs because of the activation of the PI3K signaling cascade. Because activation of PI3K signaling leads to feedback inhibition of insulin receptor substrate-2 (IRS2) expression, an upstream activator of PI3K, we therefore anticipated that IRS2 expression would be low in tumors that lack PTEN. Surprisingly, however, an elevation of IRS2 was often detected in tumor samples in which PTEN levels were compromised. To determine the potential contribution of Irs2 to tumor progression, Pten$^{+/-}$ mice were crossed with Irs2$^{+/-}$ mice. Deletion of Irs2 did not affect the initiation of neoplasia found in Pten$^{+/-}$ mice but suppressed cancer cell growth, proliferation, and invasion through the basement membrane. Deletion of Irs2 also attenuated the expression of Myc in prostatic intraepithelial neoplasia in Pten$^{+/-}$ mice. In addition, the expression levels of IRS2 and MYC were highly correlated in human prostate cancer, and IRS2 could stimulate MYC expression in cultured cells. Our findings provide evidence that the PI3K-activating adaptor Irs2 contributes to tumor progression in Pten$^{+/-}$ mice by stimulating both Myc and

Deregulation of the phosphatidylinositol-3 kinase-α (PI3K)/PTEN pathway plays a central role in oncogenesis by stimulating cell proliferation, survival, invasion, and metastasis.[1–3] PTEN, which acts as a tumor suppressor by dephosphorylating the product of PI3K (the second messenger phophatidylinositol-3,4,5-triphosphate; PtdIns-3-4-5-P3), is inactivated in a wide variety of tumors.[4] *PIK3CA*, which encodes phosphatidylinositol-3 kinase-α, is also mutated in a large proportion of human cancers.[5] Mutation of *Pten* in mice results in the appearance of neoplasms in various tissues that are associated with phosphorylation of PtdIns-3-4-5-P3-dependent AKT kinase in the neoplastic component of the tissue.[6–8]

Insulin receptor (IR) and the type 1 insulin-like growth factor receptor (IGF1R) are two of the major regulators of PI3K signaling in the cell.[9] On ligand-binding, IR and IGF1R are autophosphorylated and present docking sites for the adaptor proteins IRS1 and IRS2 (insulin receptor substrates), which are phosphorylated by the receptor tyrosine kinase. The phospho-IRS proteins recruit the p85α regulatory subunit of PI3K, which activates the p110α catalytic subunit and generates PtdIns-3-4-5-P3. As a result, PDK1, AKT1, AKT2, mTOR, and p70 S6 kinase are activated. The importance of downstream components of the PI3K signaling cascade to *Pten*$^{+/-}$ tumor phenotypes has been demonstrated using either a hypomorphic mutation of *Pdk1* or a null of *Akt1*, either

of which substantially ameliorates the $Pten^{+/-}$ tumor burden.[10,11]

It also appears that *PTEN* mutant tumor phenotypes are affected by signals upstream of *PTEN*. For instance, deletion of *Pik3r1*, which encodes the inhibitory p85 regulatory subunit of PI3K-α, enhanced tumor formation in some tissues of $Pten^{+/-}$ animals.[12] In human endometrial tumors, activating mutations of *PIK3CA* and inactivating mutations of *PTEN* often occur together and lead to increased PI3K signaling.[13] These data support the idea that multiple lesions in the same pathway can increase overall signaling on the PI3K pathway to enhance tumor formation in some tissues where this is required.

Recently, Dearth and colleagues[14] have established that the PI3K-activating adaptor *IRS2* is an oncogene. IRS2 transformed human MCF10A cells *in vitro*. Transgenic expression of IRS2 in the mouse mammary gland was highly oncogenic causing multifocal invasive and metastatic cancers. IRS2 amplification and overexpression has been observed in multiple forms of human cancer.[15–18] Thus, several lines of evidence demonstrate that IRS2 is a potent oncogene in human and mouse cells.

Activation of the PI3K pathway ultimately leads to feedback inhibition by reducing the level of IRS protein.[19–22] Thus, when PTEN is down-regulated by either RNAi or genetic inactivation in experimental tissue culture models, less IRS2 is expressed.[23,24] As one would expect, stable overexpression of PTEN leads to up-regulation of IRS2. Contrary to our expectations, we show in this report that IRS2 protein levels are in many instances up-regulated in tumors in which PTEN is inactivated.

To explore the contribution of an upstream-activating adaptor of PI3K to tumorigenesis in $Pten^{+/-}$ mice, we tested the possibility that *Irs2*, which encodes a PI3K-activating adaptor, could contribute to tumor progression in $Pten^{+/-}$ mice. We found that deletion of *Irs2* suppressed the growth, proliferation, and invasion of $Pten^{+/-}$-related neoplasia to varying degrees depending on the anatomical site. Moreover, by examining mouse and human tumor cells we showed that IRS2 is required for MYC up-regulation and is often up-regulated with MYC in cancer. Thus, our results demonstrate for the first time that a stimulatory signaling factor upstream of PI3K plays an important role in tumor progression driven by heterozygous germline mutation of *Pten*.

Materials and Methods

Mice

$Pten^{+/-8}$ and $Irs2^{+/-25}$ mice were bred to generate a cohort of mice that was heterozygous for *Pten* and wild type, heterozygous, or null for *Irs2*. When mice were sacrificed because of disease, controls to study the influence of *Irs2* mutation were sacrificed at the same time for comparison. Because $Irs2^{+/-}$ mice survived longer than $Irs2^{-/-}$ mice, we were able to observe this genotype longer.

Before sacrifice, mice were routinely given bromodeoxyuridine (BrdU). The following organs were sampled for histological analysis: brain, thyroid, lung, heart, female breast, lymph nodes, spleen, gastrointestinal tract (after it was inspected for polyps), liver, pancreas, adrenal glands, kidneys, bladder, and genital tract. All tissue samples were fixed in cold (4°C) 10% buffered formalin for no longer than 24 hours, embedded in paraffin, and sectioned for histological (hematoxylin and eosin) and immunohistochemical analyses. In histological evaluations, epithelial tissue adjacent to neoplastic tissue was discriminated from *in situ* neoplasia in prostate (PIN), endometrial *in situ* neoplasia (EIN), and colon adenomas. Carcinoma of the prostate (CAP) was defined by the absence of a basal cell layer around neoplastic glands.[26] Endometrial carcinoma was defined by considering either vascular tumor invasion or extension of the neoplastic glands into the myometrium, whereas the criterion for progression of colon adenoma to carcinoma was its extension into the colonic submucosa. Squamous cell carcinomas of the skin and mammary carcinomas were always invasive with infiltration of the underlying dermis or mammary fat. Pheochromocytomas were determined by the size of the adrenal medulla. The diameter of the adrenal medulla was divided by that of the adrenal cortex (M/C ratio). If this M/C ratio was greater than 1 (mean M/C ratio $\pm$ SD is 0.50 $\pm$ 0.14 for $Pten^{+/+}$ male and 0.28 $\pm$ 0.11 in $Pten^{+/+}$ female mice), the adrenal medulla was considered neoplastic.

Human Prostate Cancer

High-density tissue arrays (Cytokinetics Inc., South San Francisco, CA) obtained from formalin-fixed, paraffin-embedded specimens contained 96 cases of prostate cancer with defined tumor stage and grade. At least two foci of each case were sampled. Thirty-five samples of benign prostatic hyperplasia or prostate tissue without disease served as baseline controls for immunohistochemical analysis.

Immunohistochemistry and Fluorescent in Situ Hybridization (FISH)

Antibodies (Abs) used include anti-IRS2 polyclonal Ab (1:50; Upstate, Charlottesville, VA), anti-Pten monoclonal Ab (1:200; Cell Signaling Technology, Danvers, MA), anti-BrdU monoclonal Ab (1:100; BD Biosciences, San Jose, CA), anti-phosphoAkt (Ser473) monoclonal Ab (1:100, Cell Signaling Technology), anti-phosphoS6 (Ser235/236) ribosomal protein polyclonal Ab (1:50, Cell Signaling Technology), anti-phospho Erk$_{1,2}$ (Thr202/Tyr204) monoclonal Ab (1:100, Cell Signaling Technology), anti-Myc polyclonal Ab (N-262) (1:100; Santa Cruz Biotechnology Inc., Santa Cruz, CA), anti-E-cadherin monoclonal Ab (1:100; Calbiochem, San Diego, CA), anti-cytokeratin monoclonal Abs (AE1/AE3) (1:50; Chemicon Int. Inc., Temecula, CA), and anti-p63 monoclonal Ab (1:500, BD Biosciences). Antigen retrieval in 0.01 mol/L citrate buffer (pH 6.0) or in 0.01 mol/L ethylenediaminetetraacetic acid (pH 8.0) for Myc was performed in all cases. Incubation with the primary Ab was performed overnight at 4°C and

the target antigen was visualized with the conventional avidin-biotin-peroxidase system (Vectastain ABC kit; Vector Laboratories, Burlingame, CA) using 3,3′-diaminobenzidine as a substrate, yielding a brown reaction product. Human tissue arrays were stained for IRS2, PTEN, and MYC protein with the same antibodies used for mouse tissues. For FISH, the BAC RP11-150I8 probe for *IRS2* and LSI 13 SGDNA for Rb were used to detect copy numbers in tumor cell lines and 24 prostate carcinomas.[27]

Quantitative Tissue Evaluation

The extent of prostatic intraepithelial neoplasia (PIN) was expressed as the percentage of glandular profiles with PIN divided by the total number of profiles in the dorsolateral lobes of the prostate, whereas extent of EIN was expressed as the average number of glands altered by EIN per uterine cross section (at least six cross sections were averaged per case). The area of the adrenal medullae (M) and cortex (C) was measured by an automated image analysis system and expressed as M/C ratio. For each prostatic gland dorsolateral lobe and adrenal medulla, the number of BrdU-positive nuclei (ie, proliferation index), Pten-positive cells, Myc-positive nuclei, $pErk_{1,2}$-positive nuclei, pAkt-positive cells (surface and nuclear), and pS6-positive cells (cytoplasmic) were evaluated and expressed as percentage of total cell number (at least 300 cells were counted). Each sample in tissue arrays of human prostate cancer was evaluated semiquantitatively. Scoring for IRS2 was based on its cytoplasmic distribution whereas for MYC it was based on the presence of staining in cell nuclei. A score of 0 and 1 represents weak staining in <15% (0) or >15% (1) of the cells, whereas scores of 2 and 3 represent strong labeling in <15% (2) or >15% (3) of the cells. Prostate cancers with PTEN loss occurring in more than 95% of cancer cells received a score of 2, ie, complete PTEN loss. If PTEN loss occurred in more than 50% of cancer cells the score was 1, ie, partial loss, and 0 if more than 50% of cancer cells showed an immunohistochemical signal for PTEN.

Luciferase Reporter Assays

For transfection, 293 cells were plated for 24 hours in six-well plates (5×10^5 cells per well). ExGen 500 (MBI Fermentas, Glen Burnie, MD) was used as a transfection reagent. Each reaction included 250 ng of the TRAIL luciferase reporter (obtained from J. Millbrant of Washington University, St. Louis, Missouri), 100 ng of the TK Renilla control reporter (Promega, Madison, WI), and additional plasmids as indicated.[28] The pCEP4-*PTEN* vector was described previously.[29] Reporter assays were done 48 hours after transfection using a dual luciferase assay system (Promega). Firefly luciferase activities were normalized using the corresponding Renilla luciferase standard. Transfections were performed in triplicate.

Transfections, Lysate Preparation, and Western Blotting

All cell lines were obtained from American Tissue Culture Collection (Manassas, VA) and grown as recommended. MCF10A cells were transfected using electroporation by nucleofection (Amaxa Biosystems, Gaithersburg, MD) with 2 μg of either pCDNA3 or pCDNA3-*IRS2* along with 250 ng of eGFP-N1 and 100 nmol/L of each RNAi oligomer. Lysates were prepared 24 hours after transfection. Electrophoresis and Western analysis of proteins were performed using antibodies described above.
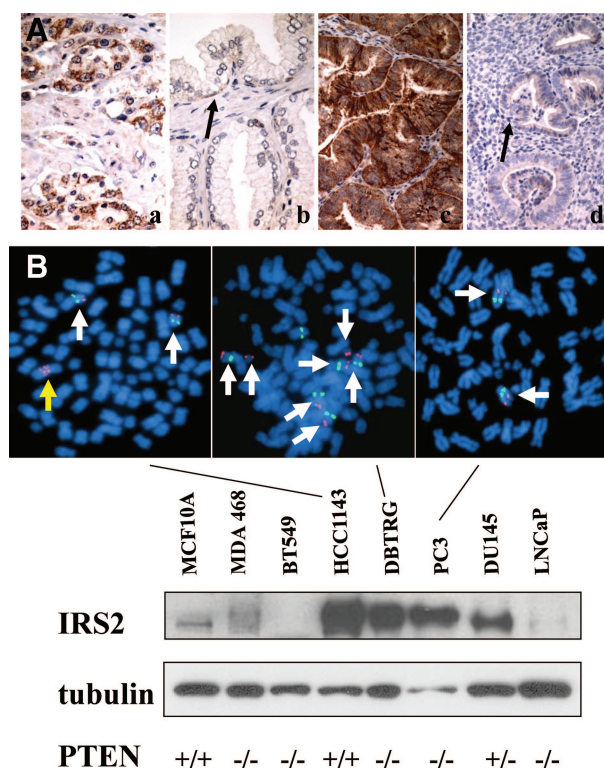
Figure 1. IRS2 is elevated in $Pten^{+/-}$ neoplasia of the prostate and uterus and in tumor cell lines. **A:** Immunohistochemical analysis of IRS2 protein expression in human prostate cancer (**a**), adjacent area of hyperplasia (**b**), human endometrial cancer (**c**), and adjacent proliferative endometrium (**d**). IRS2 expression is increased in cancer relative to nonneoplastic adjacent epithelium. Basal epithelial cells of the prostate and proliferative endometrium show light IRS expression (**black arrows**). **B:** Protein lysates were generated from human tumor cell lines under recommended growth conditions and immunoblots were examined for IRS2 protein and tubulin. IRS2 protein levels varied greatly among lines. IRS2 protein levels were relatively low in MCF10A (immortal normal breast cell line), MDA-MB-468, BT549, and LNCaP, and much higher in HCC1143, DBTRG, PC3, and DU145. Cell lines not shown also had low levels of IRS2 protein. FISH of the lines showed that HCC1143 and DBTRG had increased copies of the *IRS2* gene (red), whereas DU145 has two copies (**arrows**). Probing of PC3 also showed normal *IRS2* copy number (data not shown). A RB FISH probe (green) was used as a control because it is also on chromosome 13q. Metaphase spreads are shown that indicate that HCC1143 has a homogeneously staining region (**yellow arrow**) for *IRS2* in addition to two other copies (**white arrows**) and that DBTRG has at least seven copies of *IRS2*, five of which are attributable to an increase in the number of copies of chromosome 13q. PTEN genotypes: MCF10A wild type (+/+); DU145 heterozygous mutant (+/−); HCC1143 wild type (+/+); MDA-MB-468, BT549, DBTRG, PC-3, LNCaP both alleles mutated and/or deleted (−/−). Original magnifications, ×400 (**A**).

Table 1. Incidence of Invasive Neoplasms in Percent (Absolute Number in Parentheses) of Breast, Skin, Prostate, Endometrium, and Colon in *Pten*^{+/−} Mice

Study period Genotype	150 to 330 days		150 to 400 days	
	Pten^{+/−}*Irs2*^{+/+}	*Pten*^{+/−}*Irs2*^{−/−}	*Pten*^{+/−}*Irs2*^{+/+}	*Pten*^{+/−}*Irs2*^{+/−}
Males (*n*)	9	9	30	14
Colon cancer	22% (2)	0	7% (2)	0
Prostate cancer	22% (2)	0	20% (6)	29% (4)
Skin cancer	11% (1)	0	10% (3)	0
Females (*n*)	14	10	20	32
Endometrial carcinoma	7% (1)	0	10% (2)	6% (2)
Skin cancer	14% (2)	0	15% (3)	9% (3)
Breast cancer	21% (3)	0	45% (9)	19% (6)
All animals (*n*)	23	19	50	46
Incidence for invasive neoplasms[†]	43% (10)	0*	44% (22)	28% (13)

The study period ranged from 150 to 330 days to compare *Pten*^{+/−}*Irs2*^{+/+} with *Pten*^{+/−}*Irs2*^{−/−} mice and from 150 to 400 days to compare *Pten*^{+/−}*Irs2*^{+/+} with *Pten*^{+/−}*Irs2*^{+/−} mice. *Pten*^{+/+}*Irs2*^{+/+} (*n* = 16) and *Pten*^{+/+}*Irs2*^{−/−} (*n* = 12) controls never developed any neoplasms.
*$P < 0.001$ Fisher's exact test.
[†]Five mice (one *Pten*^{+/−}*Irs2*^{+/+} male, two *Pten*^{+/−}*Irs2*^{+/+} females, and two *Pten*^{+/−}*Irs2*^{+/−} females) had two invasive neoplasms (ie, prostate and skin, breast and skin, or endometrial and breast cancer), which were counted as a single event to calculate incidence.

Statistical Analysis

All values were expressed as means ± standard errors and compared statistically (Student's *t*-tests). Prevalences of rodent neoplasms or human prostate cancer staining were compared using Fisher's exact test or odds ratios.

Results

Irs2 Expression Is Often Up-Regulated in Prostate and Endometrial Neoplasia in the Setting of Loss of PTEN

We surveyed IRS2 expression in prostatectomy specimens of human prostate cancer (*n* = 16) and curettings of endometrial cancer (*n* = 17) and found that Irs2 was overexpressed relative to neighboring normal epithelium in 5 of 16 cases (31%) of prostate cancer and 7 of 17 (41%) cases of endometrioid endometrial cancer, in which strong IRS2 labeling was most prominent in well-differentiated areas with glandular differentiation (Figure 1A). Contrary to our expectation that IRS2 expression would be reduced in the setting of PTEN loss of expression, overexpression of IRS2 was often seen in the context of loss of PTEN expression in uterine tumors ($P < 0.03$) (see Supplemental Figure S1 and Table S1 at *http://ajp.amjpathol.org*). To further explore the

relationship between IRS2 and PTEN, we examined IRS2 expression in *Pten*^{+/−} PIN (*n* = 50) and EIN (*n* = 9). We found that Irs2 expression either remained unchanged or was increased relative to neighboring normal epithelium in samples that we and others have previously shown to have elevated PI3K signaling (see Supplemental Figure 2 at *http://ajp.amjpathol.org*).[30,31] The specificity of IRS2 staining was confirmed using *Irs2*^{−/−} tissues (data not shown). Moreover, IRS2 protein levels were increased in immunoblots of *Pten*^{+/−} mouse liver lysates relative to wild type (see Supplemental Figure 3 at *http://ajp.amjpathol.org*). Elevated or unchanged IRS2 in a setting of PTEN inactivation is surprising because activation of PI3K signaling because of PTEN knockout or knockdown leads to reduced IRS2 expression in fibroblasts and epithelial cells.[23,24] These data suggest that tumor and other tissues are able to bypass the feedback down-regulation of IRS2 that occurs when the PI3K pathway is activated.

To further explore this paradox, we screened prostate, breast, and glioblastoma tumor cell lines for increased expression of IRS2 because these tumor types frequently activate the PI3K pathway during tumorigenesis. High levels of IRS2 were found in the breast tumor line HCC1143 (PTEN^{+/+}), the glioblastoma line DBTRG (PTEN^{−/−}), and the prostate tumor lines PC3 (PTEN^{−/−}) and DU145 (PTEN^{+/−}) (Figure 1B). On the other hand, IRS2 expression

Table 2. Incidence of Preinvasive Neoplasms in Percent (Absolute Number in Parentheses) in *Pten*^{+/−} Mice

Study period Genotype	150 to 330 days		150 to 400 days	
	Pten^{+/−}*Irs2*^{+/+}	*Pten*^{+/−}*Irs2*^{−/−}	*Pten*^{+/−}*Irs2*^{+/+}	*Pten*^{+/−}*Irs2*^{+/−}
All animals (*n*)	23	19	50	46
Pheochromocytoma	70% (16)	47% (9)	80% (40)	83% (38)
Colon adenoma	48% (11)	58% (11)	60% (30)	76% (35)
Males (*n*)	9	9	30	14
PIN	100% (9)	77% (7)	100% (30)	100% (14)
Females (*n*)	14	10	20	32
EIN	71% (10)	70% (7)	80% (16)	81% (26)

The study period ranged from 150 to 330 days to compare *Pten*^{+/−}*Irs2*^{+/+} with *Pten*^{+/−}*Irs2*^{−/−} mice and from 150 to 400 days to compare *Pten*^{+/−}*Irs2*^{+/+} with *Pten*^{+/−}*Irs*^{+/−} mice. Noninvasive tumors were found in prostate, uterus, colon, and adrenal medulla. No statistical differences were evident.
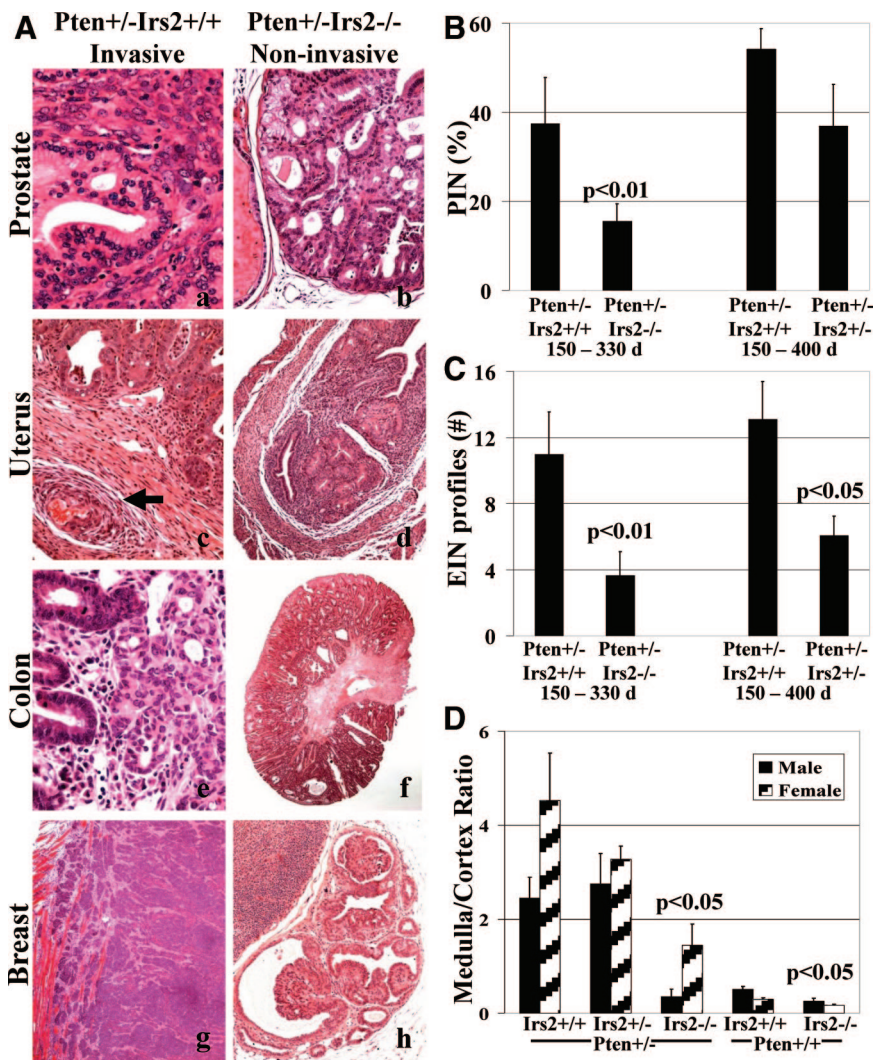
Figure 2. Deletion of *Irs2* suppresses solid tumor invasion in $Pten^{+/-}$ mice. **A:** Invasive neoplasms of prostate (**a**), endometrium with vascular invasion (**c, arrow**), colon (**e**), and breast (**g**) were observed in $Pten^{+/-}$ mice when *Irs2* was wild type, whereas the neoplasms of the same organs, prostate (**b**), endometrium (**d**), colon (**f**), and breast (**h**) remained *in situ*, ie, did not expand beyond preformed glandular structures, in $Pten^{+/-}Irs2^{-/-}$ mice. (N.B.: a single intraductal papilloma was noted among 10 $Pten^{+/-}Irs2^{-/-}$ female mice) **B** and **C:** The extent of PIN (**B**) and EIN (**C**) in $Pten^{+/-}$ mice, measured as percentage of glands involved by PIN or EIN versus total number of glandular profiles, was significantly decreased when both *Irs2* alleles were deleted in the 150- to 330-day study period [$Pten^{+/-}Irs2^{+/+}$ and $Pten^{+/-}Irs2^{-/-}$ males ($n = 9$ and 9, respectively) and for $Pten^{+/-}Irs2^{+/+}$ and $Pten^{+/-}Irs2^{-/-}$ females ($n = 14$ and 10, respectively)]. For the 150- to 400-day study period [$Pten^{+/-}Irs2^{+/+}$ and $Pten^{+/-}Irs2^{+/-}$ males ($n = 30$ and 14, respectively) and for $Pten^{+/-}Irs2^{+/+}$ and $Pten^{+/-}Irs2^{+/-}$ females ($n = 17$ and 29, respectively)] both extent of PIN (**B**) and EIN (**C**) were reduced in $Pten^{+/-}Irs2^{+/-}$ versus $Pten^{+/-}Irs2^{+/+}$ mice but this was only statistically significant ($P < 0.05$) for EIN. **D:** *Irs2* deletion suppresses adrenal medulla growth in males and females because of $Pten^{+/-}$. In adrenal glands medulla to cortex ratio (M/C ratio) was significantly reduced ($P < 0.05$) in $Pten^{+/-}Irs2^{-/-}$ but not in $Pten^{+/-}Irs2^{+/-}$ mice versus $Pten^{+/-}Irs2^{+/+}$ controls. Original magnifications: ×200 (**a, b, c, e**); ×100 (**d, f, g, h**).

was relatively low in MCF10A (PTEN$^{+/+}$), MDA-MB-468 (PTEN$^{-/-}$), BT549 (PTEN$^{-/-}$), and LNCaP (PTEN$^{-/-}$)[32] (for HCC1143 PTEN is wild-type diploid, Wellcome Trust Sanger Institute Cancer Genome Project Copy Number Analysis). To examine the basis for IRS2 overexpression, a bacterial artificial chromosome containing *IRS2*, we used FISH to assess potential gene copy number changes. Increased copy number was detected in two of the lines, HCC1143 and DBTRG. HCC1143 possessed a homogeneously staining region of *IRS2* in addition to two other unlinked *IRS2* copies, whereas the second line had seven copies of *IRS2*. No copy number changes were seen in lines PC3 or DU145, which also overexpressed IRS2 (Figure 1B and data not shown). Overexpression or unchanged expression of IRS2 occurred in cells that lacked or were haploinsufficient for PTEN, which suggests that IRS2 could contribute to tumor formation in a setting of PTEN inactivation.

Irs2 Deletion Suppresses Tumor Invasion in a Variety of Mouse Organs

To determine the contribution of excess *Irs2* expression in $Pten^{+/-}$ mouse tumor development, we generated two

groups of mice, one to study the relationship between $Pten^{+/-}$ and $Irs2^{-/-}$ from 150 to 330 days and the other to study the relationship between $Pten^{+/-}$ and $Irs2^{+/-}$ from 150 to 400 days (Tables 1 and 2). Although $Pten^{+/-}Irs2^{+/+}$ mice developed invasive carcinomas in a variety of organs, $Pten^{+/-}Irs2^{-/-}$ mice did not (($P < 0.01$) (Table 1; Figures 2A and 3A). On the other hand, $Pten^{+/-}Irs2^{+/-}$ mice developed carcinomas at frequencies similar to $Pten^{+/-}Irs2^{+/+}$. All invasive neoplasms in the prostate and, to a lesser extent, in other organs showed epithelial-mesenchymal transition, with malignant cells assuming a spindle shape and reduced labeling for E-cadherin and cytokeratin together with constitutive nuclear localization of phosphoserine-473-Akt. (Figure 3B). The status of *Irs2* did not affect the frequency of occurrence of preinvasive neoplasia of the prostate, uterus, adrenal medulla, and colon (Table 2; Figures 2A and 3A).

Irs2 Deletion Suppresses Extent of Prostate, Endometrial, and Adrenal Medulla Neoplasia

To assess the contribution of *Irs2* to the extent of *in situ* neoplasia in $Pten^{+/-}$ mice, we analyzed tissues from
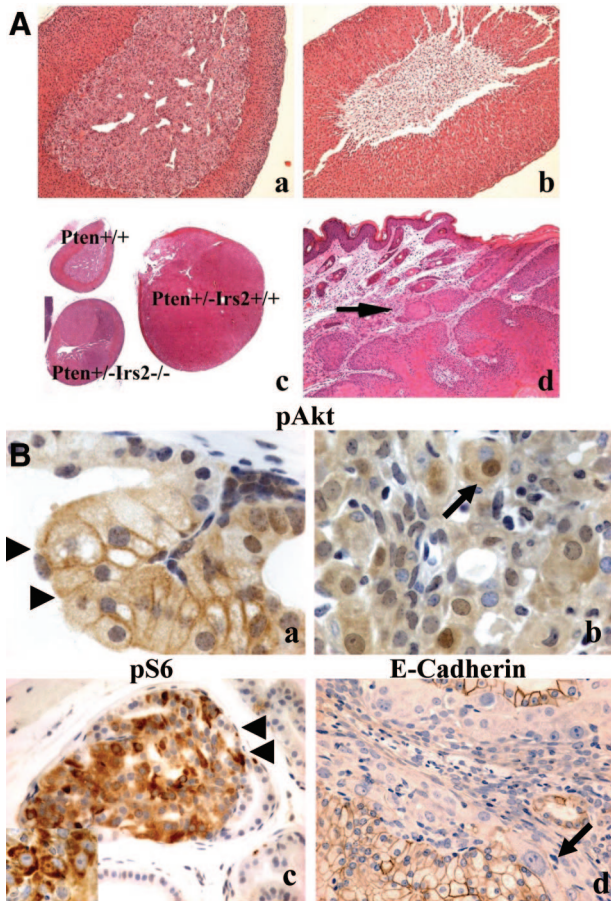
Figure 3. Pathology found in *Irs2*$^{-/-}$, *Pten*$^{+/-}$, and compound mutant animals. **A:** Adrenal glands of *Pten*$^{+/+}$*Irs2*$^{+/+}$ (**a**) and *Pten*$^{+/+}$*Irs2*$^{-/-}$ female mice (**b**) with replacement of adrenal medulla by fat in the latter genotype. The adrenal medulla was rescued in *Irs2*$^{-/-}$ mice, when they were heterozygous for *Pten* deletion (**c**). Pheochromocytomas in *Pten*$^{+/-}$*Irs2*$^{-/-}$ mice, however, never reached the same size as those seen in *Pten*$^{+/-}$*Irs2*$^{+/+}$ controls (**c**). **c:** An adrenal gland of a wild-type littermate is included for size comparison. **d:** Invasive squamous cell carcinoma (**arrow**) was only seen in *Pten*$^{+/-}$ mice when at least one *Irs2* allele was intact. **B:** Prostate carcinoma found in *Pten*$^{+/-}$*Irs2*$^{+/+}$ has altered localization of phospho-AKT and epithelial-mesenchymal transition. PIN (**a**, **arrowheads**) and invasive prostate cancer (**b**) of *Pten*$^{+/-}$ mice labeled for phospho Akt(473) (pAkt) (**a**, **b**), phospho-235/236-S6 ribosomal protein (pS6) (**c**) to demonstrate activation of the PI-3 kinase pathway with up-regulation of pAkt along the cell surface at the transition between PIN and nonneoplastic epithelium (**a**), and increased labeling for pS6 in both PIN (**c**) and invasive cancer (**inset in c**). Loss of E-cadherin staining (**d**) in invasive carcinoma is consistent with epithelial-mesenchymal transition. This phenomenon, which was near complete in our mouse model, resulted in only rare E-cadherin-positive prostate cancer cells remaining (**arrow in d**). It was accompanied by constitutive staining for pAkt in the cell nucleus (**arrow in b**). Original magnifications: ×100 (**Aa**, **Ab**, **Ad**); ×20 (**Ac**); ×100 [**Ba**, **Bb**, **Bc** (**inset**)]; ×400 (**Bc**, **Bd**).

Pten$^{+/-}$*Irs2*$^{-/-}$, *Pten*$^{+/-}$*Irs2*$^{+/-}$, and age-matched *Pten*$^{+/-}$*Irs2*$^{+/+}$ animals taken from the 150- to 330-day and 150- to 400-day cohorts. Although the *Irs2*$^{-/-}$ genotype did not decrease the occurrence of *in situ* neoplasia found in *Pten*$^{+/-}$ mice, it did diminish its extent in the prostate, uterus, and adrenal medulla relative to *Pten*$^{+/-}$*Irs2*$^{+/+}$ controls ($P < 0.01$, <0.01, and <0.05, respectively) (Figure 2, B–D; Figure 3A). For the *Pten*$^{+/-}$*Irs2*$^{+/-}$ animals, there was also less extensive EIN in mice ($P < 0.05$), and this trend was also seen for PIN and pheochromocytoma. In *Pten*$^{+/+}$*Irs2*$^{-/-}$ mice, part or all of the medulla was replaced by fibroadipose tissue (Figure 3A), decreasing
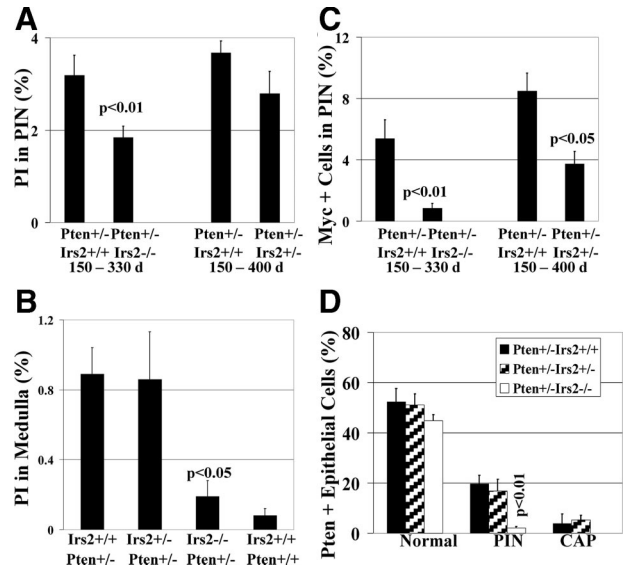
Figure 4. Deletion of Irs2 suppresses epithelial growth, proliferation, and Myc. **A:** Proliferation index (PI) determined by BrdU immunolabeling of PIN. PI is significantly reduced in *Pten*$^{+/-}$*Irs2*$^{-/-}$ mice ($P < 0.01$) and trends toward reduction in *Pten*$^{+/-}$*Irs2*$^{+/-}$ mice when compared to the *Pten*$^{+/-}$*Irs2*$^{+/+}$ group throughout respective study periods. Invasive prostate cancer (not shown) had the highest proliferation index (13.1 ± 1.9%). **B:** *Irs2* deletion suppresses adrenal medulla proliferation attributable to *Pten*$^{+/-}$. In adrenal medulla proliferation index is significantly reduced ($P < 0.05$) in *Pten*$^{+/-}$*Irs2*$^{-/-}$ but not in *Pten*$^{+/-}$*Irs2*$^{+/-}$ mice versus *Pten*$^{+/-}$*Irs2*$^{+/+}$ controls. **C:** Nuclear Myc immunolabeling is significantly reduced in *Pten*$^{+/-}$*Irs2*$^{-/-}$ ($P < 0.01$) and *Pten*$^{+/-}$*Irs2*$^{+/-}$ ($P < 0.05$) mice compared *Pten*$^{+/-}$*Irs2*$^{+/+}$ controls. Invasive prostate cancer (9.38 ± 1.97%) has the highest number of Myc-positive cells (data not shown). **D:** Pten expression is markedly reduced in *Pten*$^{+/-}$*Irs2*$^{-/-}$ PIN lesions. Comparison of percentage of Pten-positive prostatic epithelial cells in normal tissue, PIN, and CAP of *Pten*$^{+/-}$*Irs2*$^{+/+}$, *Pten*$^{+/-}$*Irs2*$^{+/-}$, and *Pten*$^{+/-}$*Irs2*$^{-/-}$ mice. Notably, PIN of *Pten*$^{+/-}$*Irs2*$^{-/-}$ mice shows nearly complete Pten loss of expression with on average 2.1 ± 0.6% cells immunoreactive for Pten, which is a significant reduction compared to PIN in *Pten*$^{+/-}$*Irs2*$^{+/+}$ controls ($P < 0.01$).

the ratio of adrenal medulla to cortex (M/C) significantly ($P < 0.05$) (Figure 2D). *Pten* haploinsufficiency rescued this adrenal phenotype.

Deletion of Irs2 Reduces Proliferation in PIN and Adrenal Medulla

To better understand the basis for the reduced tumor size, we examined the prostate and adrenal lesions for their level of proliferation. The proliferation index of PIN (Figure 4A) was decreased significantly when both alleles of *Irs2* were deleted. Measurement of the proliferative index of adrenal medullas (Figure 4B) disclosed an approximately equal mean proliferation index for *Pten*$^{+/-}$*Irs2*$^{+/+}$ (0.89 ± 0.15%) and *Pten*$^{+/-}$*Irs2*$^{+/-}$ (0.86 ± 0.27%), which is more than 10-fold elevated ($P < 0.05$) over *Pten*$^{+/+}$*Irs2*$^{+/+}$ controls (0.08 ± 0.04%). In *Pten*$^{+/-}$*Irs2*$^{-/-}$ adrenal medullas, the proliferation index is nearly fivefold lower than in animals with at least one functional *Irs2* gene (0.19 ± 0.09%, $P < 0.05$) and not significantly distinct from wild-type controls ($P = 0.39$).

Deletion of Irs2 Decreases Myc in PIN Lesions

To identify a possible intermediate of *Irs2* that was responsible for increased tumor proliferation, we studied
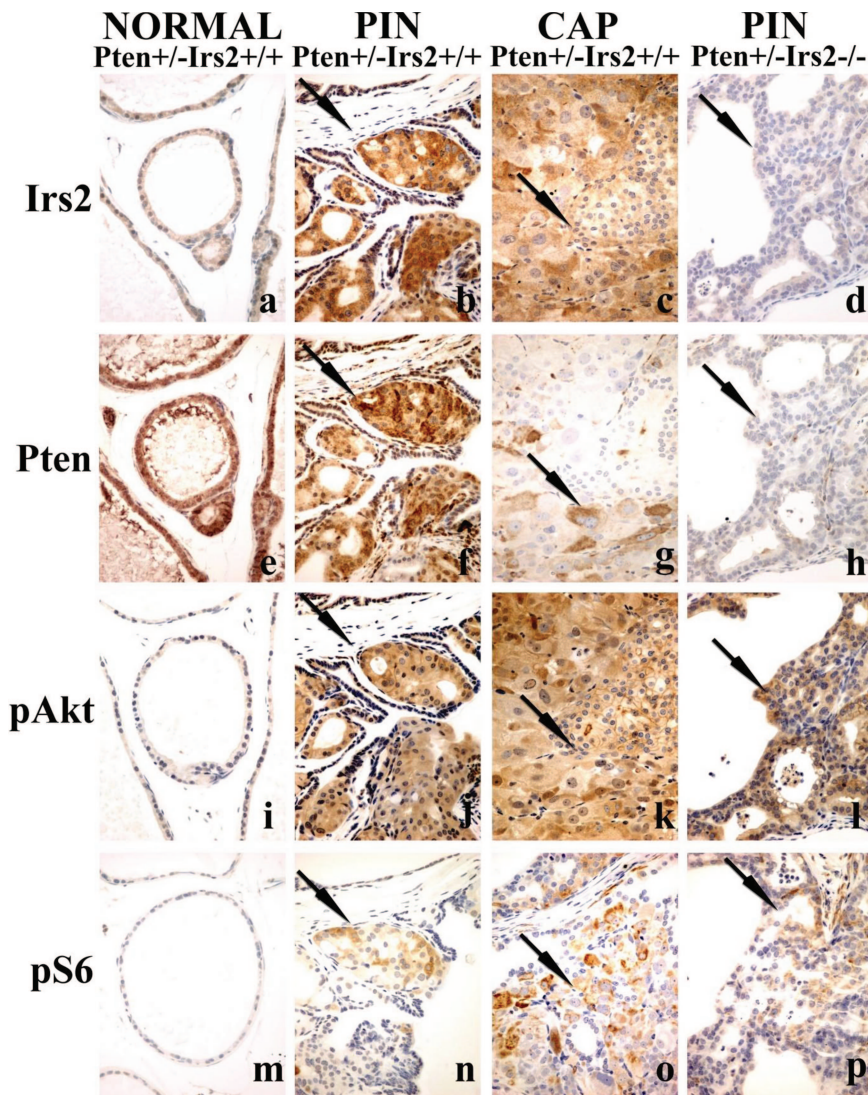
Figure 5. PI3K pathway components and signaling in PIN lesions. Immunoperoxidase staining of adjacent sections for Irs2 (**a–d**), Pten (**e–h**), pAkt (phosphoserine 473) (**i–l**), and pS6 (phosphoserines 235 and 236) (**m–p**) of prostates of $Pten^{+/-}$ transgenic mice focusing on nonneoplastic tissue (NORMAL) (**a, e, i, m**), PIN (**b, f, j, n**), or CAP (**c, g, k, o**) of $Pten^{+/-} Irs2^{+/+}$ mice or PIN of $Pten^{+/-} Irs2^{-/-}$ mice (**d, h, l, p**); the latter did not develop CAP. The nonneoplastic tissue is stained weakly (negative) for Irs2 (**a**), strongly positive for Pten (**e**), and negative for pAkt (**i**) and pS6 (**m**) suggesting quiescent PI3K signaling. *Irs2* is up-regulated in both PIN (**arrow** in **b**) and CAP (**arrow** in **c**), whereas Pten staining gradually decreases in PIN (**arrow** in **f** indicates positive cells) and is virtually absent in CAP (**arrow** in **g** indicates positive cell) in $Pten^{+/-} Irs2^{+/+}$ mice together with significant up-regulation of PI3K signaling with high levels of pAkt (**j, k**) and pS6 (**n, o**) in PIN and CAP. PIN of $Pten^{+/-} Irs2^{-/-}$ mice (see negative Irs2 labeling in **d**) shows significantly more Pten loss (**arrow** in **h**, see also Figure 4D) than the $Pten^{+/-} Irs2^{+/+}$ controls (**f**). Compared to normal, however, pAkt (**l**) and pS6 (**p**) levels in PIN of $Pten^{+/-} Irs2^{-/-}$ mice are still elevated. Arrows in d, h, l and p show PIN in $Pten^{+/-} Irs2^{-/-}$ mice. **Arrows** (**b, f, j, n**) show PIN and prostate carcinoma (**c, g, k, o**) in $Pten^{+/-} Irs2^{+/+}$. Original magnifications, ×400.

Myc, which plays a pivotal role in cell-cycle progression and cooperates with members of the PI3K pathway.[33,34] Concomitant with the decrease in proliferation, *Irs2* deletion decreased nuclear accumulation of Myc in a dose-dependent manner (Figure 4C), from 8.5 ± 1.2% positive cell nuclei in PIN of $Pten^{+/-}$ controls to 3.7 ± 0.8% in $Pten^{+/-} Irs2^{+/-}$ and 0.8 ± 0.3% in $Pten^{+/-} Irs2^{-/-}$ (5.4 ± 1.2% in age-matched $Pten^{+/-}$ mice for comparison with $Pten^{+/-} Irs2^{-/-}$). Elevation of nuclear Myc in invasive cancer (9.4 + 2.0%) was similar to the level of $Pten^{+/-} Irs2^{+/+}$ PIN.

Effect of Irs2 Deletion on PI3K/PTEN Pathway in Murine PIN

We next examined $Pten^{+/-} Irs2^{+/+}$ and $Pten^{+/-} Irs2^{-/-}$ prostate lesions for markers of the PI3K pathway using immunohistochemistry. IRS2, pAKT, and pS6 levels were elevated in PIN and CAP from $Pten^{+/-} Irs2^{+/+}$ mice (Figure 5). Compared to nonneoplastic prostate glands, Irs2, p-Akt, and p-S6 kinase staining was consistently stronger

in PIN ($n = 51$) and invasive prostate cancer ($n = 10$) of $Pten^{+/-}$ mice relative to adjacent normal epithelium. Irs2 up-regulation preceded Pten loss in PIN, as in each case multiple foci of PIN labeled strongly for both Pten and Irs2 ($n = 44$). All invasive prostate cancers lacked Pten in the overwhelming majority of cells and exhibited a high and widespread signal for Irs2, p-Akt, and p-S6. There was a marked reduction in Pten staining ($P < 0.01$) in $Pten^{+/-} Irs2^{-/-}$ PIN lesions ($n = 7$) relative to the $Pten^{+/-} Irs2^{+/+}$ controls ($n = 9$) (Figure 4D and Figure 5), whereas no differences in p-AKT or p-S6 were detected, suggesting that loss of PTEN expression in PIN is not able to compensate for the lack of *Irs2* with regard to tumor growth.

IRS2, PTEN, and MYC Expression in Human Prostate Cancer

Based on our mouse and human cell line studies, tissue arrays containing 96 prostatic adenocarcinomas, 14 benign prostatic hyperplasias, and 21 normal prostate samples were labeled for IRS2, PTEN, and MYC. Weak cyto-
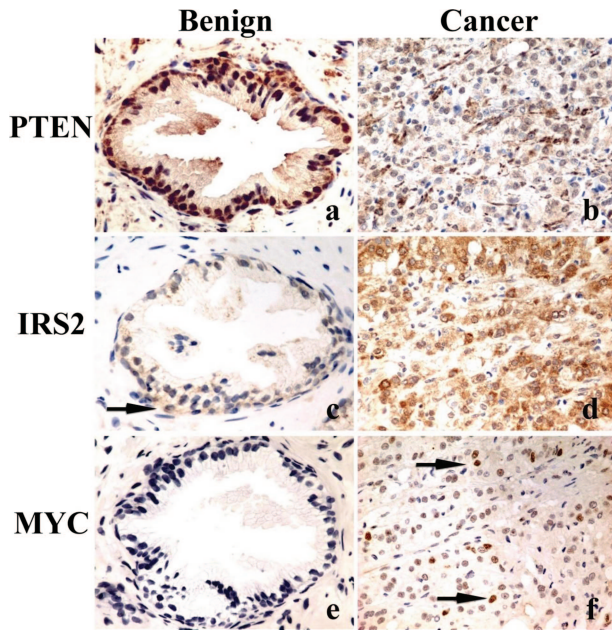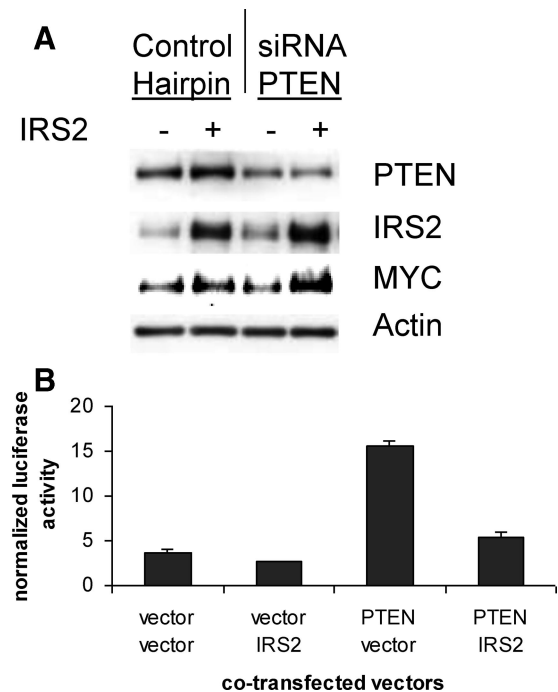
Figure 6. PTEN, MYC, and IRS2 expression in human prostate. Human prostate with benign glandular hyperplasia (**a**, **c**, **e**) and invasive prostate cancer (**b**, **d**, **f**) labeled for PTEN (**a**, **b**), IRS2 (**c**, **d**), and MYC (**e**, **f**). PTEN shows a strong signal in benign prostatic glands (**a**) but is lost in most invasive cancer cells (**b**). Inversely, IRS2 shows a weak signal in few benign prostatic basal cells (**arrow** in **c**) and strong labeling of invasive cancer cells (**d**). Nuclear c-MYC was absent in benign prostatic glands (**e**), but strongly up-regulated in a fraction of invasive prostate cancer cells (**arrows** in **f**). Original magnifications, ×400.

Figure 7. IRS2 stimulates the expression of MYC and PI3K signaling. **A:** Expression vectors (IRS2 and empty vector) and RNAi (PTEN and GFP) oligos were electroporated into MCF10A cells to determine their effect on MYC. Western blots of lysates were probed with indicated antibodies. Transfected IRS2 increased the level of MYC expression slightly (11%), whereas PTEN RNAi did not. IRS2 and PTEN together increased MYC substantially (52%). **B:** IRS2 inhibits TRAIL promoter activation by PTEN. The 293 cells were transfected with the TRAIL-luciferase and TK-renilla luciferase promoters along with either PTEN, IRS2 expression vectors, or the appropriate empty vector control.

plasmic staining for IRS2 (14 of 35 nonneoplastic samples), partial loss of PTEN (10 of 35 samples), and weak nuclear MYC labeling (2 of 35 samples) was present in benign prostatic hyperplasias. Only prostate cancers showed complete PTEN loss (24%), or a strong IRS2 signal (30%) and strong nuclear MYC (42%) immunolabeling (Figure 6; Table 2). No significant relationship between IRS2 and PTEN loss was noted ($P = 0.31$, Fisher's exact test) (Table 3). Conversely, the odds for nuclear accumulation of MYC occurring in strongly IRS2-expressing carcinomas was raised to 3.83 versus 0.34 for those with no or low IRS2 ($P < 0.00001$, Fisher's exact test, odds ratio = 11.3). Examination of IRS2 copy number in 24 prostate cancers by FISH found no cases with more than four copies of IRS2, suggesting that copy number alterations are not the cause of IRS2 overexpression in prostate carcinoma (data not shown).

IRS2 Stimulates MYC Expression and PI3K Signaling in Vitro

In addition to its role in PI3K signaling, our data suggest that increased IRS2 could contribute to tumor progression through the stimulation of MYC expression and proliferation. MCF10A cells, which are derived from normal breast epithelium, were electroporated with an IRS2 expression vector and siRNA to PTEN. Transfection of an IRS2 expression vector but not PTEN RNAi was able to increase modestly the level of MYC protein. Interestingly, the combination of CMV-IRS2 with PTEN siRNA appeared to substantially stimulate MYC expression (Figure 7A). A well-established quantitative method for measuring PI3K signaling is to use a luciferase reporter for FOXO transcription factors, which are regulated by AKT phosphor-

Table 3. Analysis of IRS2, PTEN, and MYC Expression in Human Prostate Carcinoma

		PTEN			Nuclear MYC*		
		Loss	No loss	All	Low	High	All
IRS2	Low	18	49	67 (70%)	50	17	67 (70%)
	High	5	24	29 (30%)	6	23	29 (30%)
	All	23 (24%)	73 (76%)	96	56 (58%)	40 (42%)	96

*IRS2 correlates with nuclear MYC ($P < 0.00001$) Fisher's exact test.

ylation.[35] To test that increasing the amount of IRS2 is able to regulate PI3K signaling in the presence of fixed levels of extracellular growth factors, we tested the ability of transfected IRS2 to repress PTEN activation of the FOXO-dependent TRAIL promoter.[28] Increased IRS2 was able to repress the PTEN-dependent activation of the TRAIL reporter as expected (Figure 7B).

Discussion

The anticipated feedback repression of IRS2 expression because of PI3K pathway activation was not observed in tumors harboring deficits in PTEN.[23,24] Instead, we have seen that IRS2 is increased or unchanged in the setting of PTEN inactivation in human carcinoma, several human tumor cell lines, and in mouse $Pten^{+/-}$ neoplasia (Figures 1 and 6; Supplemental Figures 1 and 2, see *http://ajp. amjpathol.org*). Consistent with the idea that IRS2 contributes to PTEN-dependent tumor development, deletion of *Irs2* suppressed the extent and proliferative activity of neoplasia in $Pten^{+/-}$ mice (Figures 2 to 4). Similar results have also been obtained in sarcoma in which PTEN deletion may occur in the setting of increased IRS2 expression.[18]

Our findings are consistent with the already ample evidence that *Irs2* deletion affects cell proliferation in nervous and endocrine systems.[36–39] *Irs2*-deficient mice are severely diabetic because they are incapable of generating a sufficient amount of β cells,[40] have smaller brains because of 50% reduction of neuronal growth,[41] and lack the normal number of photoreceptors in the retina.[42] In the current study, we have extended these observations by finding that another neuroendocrine tissue, the adrenal medulla, is lacking in *Irs2*-deficient mice (Figure 3A). In agreement with previous studies of $Irs2^{-/-}$ diabetic mice in which β-cell mass was restored in a $Pten^{+/-}$ setting,[25] *Pten* haploinsufficiency rescued $Irs2^{-/-}$ adrenal cell mass, and the majority of $Pten^{+/-}$ $Irs2^{-/-}$ females even developed pheochromocytomas.

Analysis of serial sections of $Pten^{+/-}$ prostate neoplasia showed minimally altered expression of Pten, overexpression of Irs2, and activation of signaling through the Akt/TSC/mTor/p70[s6K] pathway (Figure 5). Moreover, we found that IRS2 was able to regulate a FOXO-dependent promoter in the presence of PTEN, demonstrating their antagonistic nature on the PI3K/AKT/FOXO pathway in a setting of constant receptor activation (Figure 7). Together, these data suggest that up-regulation of IRS2 in the setting of *PTEN* haploinsufficiency contributes to AKT pathway activation in a cell. Surprisingly, pAkt and pS6 were not reduced by *Irs2* deletion in prostate neoplasia. Pten, however, was reduced in these *in situ* lesions, suggesting that reduction of Pten could partially compensate for the lack of *Irs2* with respect to signal activation and neoplastic transformation but could not achieve the same proliferative stimulus observed when the *Irs2* gene was intact (Figure 4D).

MYC is an oncogene that is up-regulated in proliferating cells and stimulates cell growth and DNA synthesis.[33,43–45] In our studies, we have observed a close relationship between IRS2, MYC, and DNA synthesis. A dose effect for the *Irs2* deletion was observed for tumor proliferation and Myc accumulation in neoplasia of $Pten^{+/-}$ mice (Figure 4C). Similarly, IRS2 was able to alter the level of MYC in human tissue culture experiments in the setting of PTEN partial knockdown and correlated with MYC in prostate cancer (Figures 6 and 7; Table 3). Surprisingly, however, loss of PTEN did not correlate with MYC in any of these studies. These data together indicate that despite being on the same pathway, IRS2 and PTEN are not completely overlapping in their function. Moreover, our data suggest that the ability of IRS2 to regulate MYC is not simply occurring through the PI3K pathway.[46,47] Recent evidence demonstrating that IRS2 can up-regulate MYC via β-catenin supports this conclusion.[14]

Biallelic deletion of *Irs2* suppressed the invasion of $Pten^{+/-}$ tumors (Table 1). One possible explanation for loss of invasiveness is that, in addition to regulating proliferation, IGF1R-IRS2 signaling controls cell functions promoting invasion such as matrix degradation by activating urokinase-like plasminogen activator[48] or matrix metalloproteinases.[49,50] Another possibility is that IRS2 activation because of binding to the $\alpha6\beta4$ integrin receptor[51] has been linked to loss of cell cohesion and subsequent increased cell motility. Moreover, analysis of $Irs2^{-/-}$ mammary tumors driven by polyoma middle T antigen has shown that they are unable to metastasize and have reduced invasiveness *in vitro*.[52] However, unlike our findings, Nagle and colleagues[52] found that *Irs2* deletion does not affect proliferation. Therefore, their data would imply that the effect of IRS2 on invasion is separable from its effect on proliferation.

Our results support a model in which two components of the PI3K/PTEN pathway (ie, PTEN, IRS2) cooperate during tumor progression. Genetic inactivation of *Irs2* led to reductions in tumor proliferation, invasion, and Myc expression in $Pten^{+/-}$ mice. Further analysis demonstrated that IRS2 was overexpressed in tumors and increased PI3K signaling and MYC expression. We conclude that optimal tumor progression because of PTEN mutation requires IRS2 for the full activation of PI3K signals, MYC expression, and cell proliferation.

Acknowledgments

References

1. Cantley LC, Neel BG: New insights into tumor suppression: PTEN suppresses tumor formation by restraining the phosphoinositide 3-kinase/AKT pathway. Proc Natl Acad Sci USA 1999, 96:4240–4245
2. Parsons R: Human cancer, PTEN and the PI-3 kinase pathway. Semin Cell Dev Biol 2004, 15:171–176
3. Samuels Y, Diaz Jr LA, Schmidt-Kittler O, Cummins JM, Delong L, Cheong I, Rago C, Huso DL, Lengauer C, Kinzler KW, Vogelstein B, Velculescu VE: Mutant PIK3CA promotes cell growth and invasion of human cancer cells. Cancer Cell 2005, 7:561–573
4. Maehama T, Dixon JE: The tumor suppressor, PTEN/MMAC1, de-

phosphorylates the lipid second messenger, phosphatidylinositol 3,4,5-trisphosphate. J Biol Chem 1998, 273:13375–13378

5. Samuels Y, Wang Z, Bardelli A, Silliman N, Ptak J, Szabo S, Yan H, Gazdar A, Powell SM, Riggins GJ, Willson JK, Markowitz S, Kinzler KW, Vogelstein B, Velculescu VE: High frequency of mutations of the PIK3CA gene in human cancers. Science 2004, 304:554

6. Di Cristofano A, Pesce B, Cordon-Cardo C, Pandolfi PP: Pten is essential for embryonic development and tumour suppression. Nat Genet 1998, 19:348–355

7. Suzuki A, de la Pompa JL, Stambolic V, Elia AJ, Sasaki T, del Barco Barrantes I, Ho A, Wakeham A, Itie A, Khoo W, Fukumoto M, Mak TW: High cancer susceptibility and embryonic lethality associated with mutation of the PTEN tumor suppressor gene in mice. Curr Biol 1998, 8:1169–1178

8. Podsypanina K, Ellenson LH, Nemes A, Gu J, Tamura M, Yamada KM, Cordon-Cardo C, Catoretti G, Fisher PE, Parsons R: Mutation of Pten/Mmac1 in mice causes neoplasia in multiple organ systems. Proc Natl Acad Sci USA 1999, 96:1563–1568

9. LeRoith D, Roberts Jr CT: The insulin-like growth factor system and cancer. Cancer Lett 2003, 195:127–137

10. Bayascas JR, Leslie NR, Parsons R, Fleming S, Alessi DR: Hypomorphic mutation of PDK1 suppresses tumorigenesis in PTEN(+/−) mice. Curr Biol 2005, 15:1839–1846

11. Chen ML, Xu PZ, Peng XD, Chen WS, Guzman G, Yang X, Di Cristofano A, Pandolfi PP, Hay N: The deficiency of Akt1 is sufficient to suppress tumor development in Pten+/− mice. Genes Dev 2006, 20:1569–1574

12. Luo J, Sobkiw CL, Logsdon NM, Watt JM, Signoretti S, O'Connell F, Shin E, Shim Y, Pao L, Neel BG, Depinho RA, Loda M, Cantley LC: Modulation of epithelial neoplasia and lymphoid hyperplasia in PTEN+/− mice by the p85 regulatory subunits of phosphoinositide 3-kinase. Proc Natl Acad Sci USA 2005, 102:10238–10243

13. Oda K, Stokoe D, Taketani Y, McCormick F: High frequency of coexistent mutations of PIK3CA and PTEN genes in endometrial carcinoma. Cancer Res 2005, 65:10669–10673

14. Dearth RK, Cui X, Kim HJ, Kuiatse I, Lawrence NA, Zhang X, Divisova J, Britton OL, Mohsin S, Allred DC, Hadsell DL, Lee AV: Mammary tumorigenesis and metastasis caused by overexpression of insulin receptor substrate 1 (IRS-1) or IRS-2. Mol Cell Biol 2006, 26:9302–9314

15. Knobbe CB, Reifenberger G: Genetic alterations and aberrant expression of genes related to the phosphatidyl-inositol-3′-kinase/protein kinase B (Akt) signal transduction pathway in glioblastomas. Brain Pathol 2003, 13:507–518

16. Parsons DW, Wang TL, Samuels Y, Bardelli A, Cummins JM, DeLong L, Silliman N, Ptak J, Szabo S, Willson JK, Markowitz S, Kinzler KW, Vogelstein B, Lengauer C, Velculescu VE: Colorectal cancer: mutations in a signalling pathway. Nature 2005, 436:792

17. Kornmann M, Maruyama H, Bergmann U, Tangvoranuntakul P, Beger HG, White MF, Korc M: Enhanced expression of the insulin receptor substrate-2 docking protein in human pancreatic cancer. Cancer Res 1998, 58:4250–4254

18. Hernando E, Charytonowicz E, Dudas ME, Menendez S, Matushansky I, Mills J, Socci ND, Behrendt N, Ma L, Maki RG, Pandolfi PP, Cordon-Cardo C: The AKT-mTOR pathway plays a critical role in the development of leiomyosarcomas. Nat Med 2007, 13:748–753

19. Paz K, Hemi R, LeRoith D, Karasik A, Elhanany E, Kanety H, Zick Y: A molecular basis for insulin resistance. Elevated serine/threonine phosphorylation of IRS-1 and IRS-2 inhibits their binding to the juxtamembrane region of the insulin receptor and impairs their ability to undergo insulin-induced tyrosine phosphorylation. J Biol Chem 1997, 272:29911–29918

20. Rameh LE, Chen CS, Cantley LC: Phosphatidylinositol (3,4,5)P3 interacts with SH2 domains and modulates PI 3-kinase association with tyrosine-phosphorylated proteins. Cell 1995, 83:821–830

21. Simpson L, Li J, Liaw D, Hennessy I, Oliner J, Christians F, Parsons R: PTEN expression causes feedback upregulation of insulin receptor substrate 2. Mol Cell Biol 2001, 21:3947–3958

22. Li J, DeFea K, Roth RA: Modulation of insulin receptor substrate-1 tyrosine phosphorylation by an Akt/phosphatidylinositol 3-kinase pathway. J Biol Chem 1999, 274:9351–9356

23. Lackey J, Barnett J, Davidson L, Batty IH, Leslie NR, Downes CP: Loss of PTEN selectively desensitizes upstream IGF1 and insulin signaling. Oncogene 2007, 26:7132–7142

24. Vivanco I, Palaskas N, Tran C, Finn SP, Getz G, Kennedy NJ, Jiao J, Rose J, Xie W, Loda M, Golub T, Mellinghoff IK, Davis RJ, Wu H, Sawyers CL: Identification of the JNK signaling pathway as a functional target of the tumor suppressor PTEN. Cancer Cell 2007, 11:555–569

25. Kushner JA, Simpson L, Wartschow LM, Guo S, Rankin MM, Parsons R, White MF: Phosphatase and tensin homolog regulation of islet growth and glucose homeostasis. J Biol Chem 2005, 280:39388–39393

26. Weinstein MH, Signoretti S, Loda M: Diagnostic utility of immunohistochemical staining for p63, a sensitive marker of prostatic basal cells. Mod Pathol 2002, 15:1302–1308

27. Jakob J, Nagase S, Gazdar A, Chien M, Morozova I, Russo JJ, Nandula SV, Murty VV, Li CM, Tycko B, Parsons R: Two somatic biallelic lesions within and near SMAD4 in a human breast cancer cell line. Genes Chromosom Cancer 2005, 42:372–383

28. Modur V, Nagarajan R, Evers BM, Milbrandt J: FOXO proteins regulate tumor necrosis factor-related apoptosis inducing ligand expression. Implications for PTEN mutation in prostate cancer. J Biol Chem 2002, 277:47928–47937

29. Li J, Simpson L, Takahashi M, Miliaresis C, Myers MP, Tonks N, Parsons R: The PTEN/MMAC1 tumor suppressor induces cell death that is rescued by the AKT/protein kinase B oncogene. Cancer Res 1998, 58:5667–5672

30. Podsypanina K, Lee RT, Politis C, Hennessy I, Crane A, Puc J, Neshat M, Wang H, Yang L, Gibbons J, Frost P, Dreisbach V, Blenis J, Gaciong Z, Fisher P, Sawyers C, Hedrick-Ellenson L, Parsons R: An inhibitor of mTOR reduces neoplasia and normalizes p70/S6 kinase activity in Pten+/− mice. Proc Natl Acad Sci USA 2001, 98:10320–10325

31. Majumder PK, Yeh JJ, George DJ, Febbo PG, Kum J, Xue Q, Bikoff R, Ma H, Kantoff PW, Golub TR, Loda M, Sellers WR: Prostate intraepithelial neoplasia induced by prostate restricted Akt activation: the MPAKT model. Proc Natl Acad Sci USA 2003, 100:7841–7846

32. Li J, Yen C, Liaw D, Podsypanina K, Bose S, Wang SI, Puc J, Miliaresis C, Rodgers L, McCombie R, Bigner SH, Giovanella BC, Ittmann M, Tycko B, Hibshoosh H, Wigler MH, Parsons R: PTEN, a putative protein tyrosine phosphatase gene mutated in human brain, breast, and prostate cancer. Science 1997, 275:1943–1947

33. de Alboran IM, O'Hagan RC, Gartner F, Malynn B, Davidson L, Rickert R, Rajewsky K, DePinho RA, Alt FW: Analysis of C-MYC function in normal cells via conditional gene-targeted mutation. Immunity 2001, 14:45–55

34. Wendel HG, Lowe SW: Reversing drug resistance in vivo. Cell Cycle 2004, 3:847–849

35. Nakamura N, Ramaswamy S, Vazquez F, Signoretti S, Loda M, Sellers WR: Forkhead transcription factors are critical effectors of cell death and cell cycle arrest downstream of PTEN. Mol Cell Biol 2000, 20:8969–8982

36. Jhala US, Canettieri G, Screaton RA, Kulkarni RN, Krajewski S, Reed J, Walker J, Lin X, White M, Montminy M: cAMP promotes pancreatic beta-cell survival via CREB-mediated induction of IRS2. Genes Dev 2003, 17:1575–1580

37. Kido Y, Nakae J, Hribal ML, Xuan S, Efstratiadis A, Accili D: Effects of mutations in the insulin-like growth factor signaling system on embryonic pancreas development and beta-cell compensation to insulin resistance. J Biol Chem 2002, 277:36740–36747

38. Kushner JA, Haj FG, Klaman LD, Dow MA, Kahn BB, Neel BG, White MF: Islet-sparing effects of protein tyrosine phosphatase-1b deficiency delays onset of diabetes in IRS2 knockout mice. Diabetes 2004, 53:61–66

39. Mohanty S, Spinas GA, Maedler K, Zuellig RA, Lehmann R, Donath MY, Trub T, Niessen M: Overexpression of IRS2 in isolated pancreatic islets causes proliferation and protects human beta-cells from hyperglycemia-induced apoptosis. Exp Cell Res 2005, 303:68–78

40. Kushner JA, Ye J, Schubert M, Burks DJ, Dow MA, Flint CL, Dutta S, Wright CV, Montminy MR, White MF: Pdx1 restores beta cell function in Irs2 knockout mice. J Clin Invest 2002, 109:1193–1201

41. Schubert M, Brazil DP, Burks DJ, Kushner JA, Ye J, Flint CL, Farhang-Fallah J, Dikkes P, Warot XM, Rio C, Corfas G, White MF: Insulin receptor substrate-2 deficiency impairs brain growth and promotes tau phosphorylation. J Neurosci 2003, 23:7084–7092

42. Yi X, Schubert M, Peachey NS, Suzuma K, Burks DJ, Kushner JA, Suzuma I, Cahill C, Flint CL, Dow MA, Leshan RL, King GL, White MF:

Insulin receptor substrate 2 is essential for maturation and survival of photoreceptor cells. J Neurosci 2005, 25:1240–1248

43. Baena E, Gandarillas A, Vallespinos M, Zanet J, Bachs O, Redondo C, Fabregat I, Martinez AC, de Alboran IM: c-Myc regulates cell size and ploidy but is not essential for postnatal proliferation in liver. Proc Natl Acad Sci USA 2005, 102:7286–7291

44. Zanet J, Pibre S, Jacquet C, Ramirez A, de Alboran IM, Gandarillas A: Endogenous Myc controls mammalian epidermal cell size, hyperproliferation, endoreplication and stem cell amplification. J Cell Sci 2005, 118:1693–1704

45. Dominguez-Sola D, Ying CY, Grandori C, Ruggiero L, Chen B, Li M, Galloway DA, Gu W, Gautier J, Dalla-Favera R: Non-transcriptional control of DNA replication by c-Myc. Nature 2007, 448:445–451

46. Sears R, Nuckolls F, Haura E, Taya Y, Tamai K, Nevins JR: Multiple Ras-dependent phosphorylation pathways regulate Myc protein stability. Genes Dev 2000, 14:2501–2514

47. Yeh E, Cunningham M, Arnold H, Chasse D, Monteith T, Ivaldi G, Hahn WC, Stukenberg PT, Shenolikar S, Uchida T, Counter CM, Nevins JR, Means AR, Sears R: A signalling pathway controlling c-Myc degradation that impacts oncogenic transformation of human cells. Nat Cell Biol 2004, 6:308–318

48. Tarbé N, Losch S, Burtscher H, Jarsch M, Weidle UH: Identification of rat pancreatic carcinoma genes associated with lymphogenous metastasis. Anticancer Res 2002, 22:2015–2027

49. Zhai GG, Malhotra R, Delaney M, Latham D, Nestler U, Zhang M, Mukherjee N, Song Q, Robe P, Chakravarti A: Radiation enhances the invasive potential of primary glioblastoma cells via activation of the Rho signaling pathway. J Neurooncol 2006, 76:227–237

50. Zhang D, Bar-Eli M, Meloche S, Brodt P: Dual regulation of MMP-2 expression by the type 1 insulin-like growth factor receptor: the phosphatidylinositol 3-kinase/Akt and Raf/ERK pathways transmit opposing signals. J Biol Chem 2004, 279:19683–19690

51. Shaw LM: Identification of insulin receptor substrate 1 (IRS-1) and IRS-2 as signaling intermediates in the alpha6beta4 integrin-dependent activation of phosphoinositide 3-OH kinase and promotion of invasion. Mol Cell Biol 2001, 21:5082–5093

52. Nagle JA, Ma Z, Byrne MA, White MF, Shaw LM: Involvement of insulin receptor substrate 2 in mammary tumor metastasis. Mol Cell Biol 2004, 24:9726–9735